

Global Lepton-Quark Neutral Current Constraint on Low Scale Gravity Model

Kingman Cheung

*Department of Physics, University of California, Davis, CA 95616 USA***Abstract**

We perform a global analysis of the lepton-quark neutral current data on the low scale gravity model, which arises from the extra dimensions. The global data include HERA neutral current deep-inelastic scattering, Drell-yan production at the Tevatron, and fermion pair production at LEPII. The Drell-yan production, due to the large invariant mass data, provides the strongest constraint. Combining all data, the effective Planck scale must be larger than about 1.15 TeV for $n = 3$ and 0.97 TeV for $n = 4$ at 95%CL.

1. Introduction

A solution to the gauge hierarchy, based on extra spacial dimensions, was recently proposed by Arkani-Hamed, Dimopoulos and Dvali [1]. They assumed the space-time is $4 + n$ dimensional, with the standard model (SM) particles living on a brane. While the electromagnetic, strong, and weak forces are confined to this brane, gravity can propagate in the extra dimensions. To solve the gauge hierarchy problem they proposed the “new” Planck scale M_S is of the order of TeV with very large extra dimensions. The size R of these extra dimensions can be as large as 1 mm, which corresponds to a compactification scale R^{-1} as low as 10^{-4} eV. The usual Planck scale $M_G = 1/\sqrt{G_N} \sim 1.22 \times 10^{19}$ GeV is related to this effective Planck scale M_S using the Gauss’s law:

$$R^n M_S^{n+2} \sim M_G^2, \quad (1)$$

where n is the number of extra dimensions. For $n = 1$ it gives a large value for R , which is already ruled out by gravitational experiments. On the other hand, $n = 2$ gives $R \lesssim 1$ mm, which is in the margin beyond the reach of present gravitational experiments.

The graviton including its excitations in the extra dimensions can couple to the SM particles on the brane with an effective strength of $1/M_S$ (instead of $1/M_G$) after summing the effect of all excitations collectively, and thus the gravitation interaction becomes comparable in strength to weak interaction at TeV scale. Hence, it can give rise to a number of phenomenological activities testable at existing and future colliders [2]. So far, studies show that there are two categories of signals: direct and indirect. The indirect signal refers to exchanges of gravitons in the intermediate states, while direct refers to production or associated production

of gravitons in the final state. Indirect signals include fermion pair, gauge boson pair production, correction to precision variables, etc. There are also other astrophysical and cosmological signatures and constraints [3]. Among the constraints the cooling of supernovae by radiating gravitons places the strongest limit on the effective Planck scale M_S of order 50 TeV for $n = 2$, which renders collider signatures for $n = 2$ uninteresting. Thus, we concentrate on $n \geq 3$.

In this work, we perform a global analysis of the lepton-quark neutral current data on the low scale gravity model. The global data include HERA neutral current deep-inelastic scattering, Drell-yan production at the Tevatron, and total hadronic, $b\bar{b}$ and $c\bar{c}$ pair cross sections at LEPII. In addition, we also include the leptonic cross sections $e^+e^- \rightarrow \mu^+\mu^-, \tau^+\tau^-$ at LEPII in our analysis. The ν -N scattering data from CCFR and NuTeV have been shown by Rizzo [2] to be very insignificant in constraining the low scale gravity, and so we shall not include this data set in our analysis. We shall see that the Drell-yan production, due to the large invariant mass data, provides the strongest constraint among the global data. By combining all data, the effective Planck scale M_S must be larger than about 1.15 TeV for $n = 3$ and 0.97 TeV for $n = 4$ at 95%CL. This is our main result.

The organization of the paper is as follows. In the next section, we shall describe each set of data used in our global analysis and derive the effect of the low scale gravity. In Sec. III, we give the numerical results and interpretations for our fits, from which we can draw the limits on the effective Planck scale.

2. Global Data

Before we come to each data set, let us first give a general expression for the square of amplitude for $e^-e^+ \rightarrow q\bar{q}$:

$$\begin{aligned} \sum |\mathcal{M}|^2 &= 4u^2 (|M_{LL}|^2 + |M_{RR}|^2) + 4t^2 (|M_{LR}|^2 + |M_{RL}|^2) \\ &+ 2\pi^2 \left(\frac{\mathcal{F}}{M_S^4} \right)^2 (t^4 - 6t^3u + 18t^2u^2 - 6tu^3 + u^4) \\ &+ 8\pi e^2 Q_e Q_q \frac{\mathcal{F}}{M_S^4} \frac{(u-t)^3}{s} \\ &+ \frac{8\pi e^2}{\sin^2 \theta_w \cos^2 \theta_w} \frac{\mathcal{F}}{M_S^4} \frac{1}{s - M_Z^2} \left[g_a^e g_a^q (t^3 - 3t^2u - 3tu^2 + u^3) + g_v^e g_v^q (u-t)^3 \right], \end{aligned} \quad (2)$$

where s, t, u are the usual Mandelstam variables, $e = \sqrt{4\pi\alpha}$ is the electromagnetic coupling constant, Q_f is the electric charge of the fermion f , θ_w is the Weinberg mixing angle, g_a^f and g_v^f are, respectively, the axial-vector and the vector Z couplings to the fermion f . The reduced amplitudes $M_{\alpha\beta}$ ($\alpha, \beta = L, R$) are

$$M_{\alpha\beta} = \frac{e^2 Q_e Q_q}{s} + \frac{e^2}{\sin^2 \theta_w \cos^2 \theta_w} \frac{g_\alpha^e g_\beta^q}{s - M_Z^2} \quad (3)$$

where

$$\begin{aligned} g_L^f &= T_{3f} - Q_f \sin^2 \theta_w, & g_R^f &= -Q_f \sin^2 \theta_w \\ g_v^f &= (g_L^f + g_R^f)/2, & g_a^f &= (g_L^f - g_R^f)/2. \end{aligned}$$

In the derivation, we have followed the notation in Han *et al.* [2] and we have taken $M_S^2 \gg s, |t|, |u|$ and in this case the propagator factor $D(s) = D(|t|) = D(|u|)$, which is given by

$$\kappa^2 |D(s)| = \frac{16\pi}{M_S^4} \times \mathcal{F}, \quad (4)$$

where the factor \mathcal{F} is given by

$$\mathcal{F} = \begin{cases} \log\left(\frac{M_S^2}{s}\right) & \text{for } n = 2, \\ \frac{2}{n-2} & \text{for } n > 2. \end{cases} \quad (5)$$

For $n \geq 3$ \mathcal{F} is always positive. The amplitude square for the crossed channels $e^\pm \stackrel{(-)}{q} \rightarrow e^\pm \stackrel{(-)}{q}$ can be obtained using the crossing symmetry.

2.a HERA neutral-current data

Both H1 and ZEUS have measured the neutral-current deep-inelastic scattering cross sections at high- Q^2 region. Despite the excess in cross section reported in early 1997, the 1997 data alone agreed well with the SM. The double differential cross section for $e^+p \rightarrow e^+X$ is given by

$$\begin{aligned} \frac{d^2\sigma}{dydQ^2} = & \sum_q \frac{f_q(x)}{16\pi} \frac{Q^2}{sy^2} \left\{ (1-y)^2 (|M_{LL}|^2 + |M_{RR}|^2) + |M_{LR}|^2 + |M_{RL}|^2 \right. \\ & + \frac{\pi^2}{2} \left(\frac{Q^2}{y} \right)^2 \left(\frac{\mathcal{F}}{M_S^4} \right)^2 (32 - 64y + 42y^2 - 10y^3 + y^4) \\ & + 2\pi e^2 Q_e Q_q \left(\frac{\mathcal{F}}{M_S^4} \right) \frac{(2-y)^3}{y} \\ & + \frac{2\pi e^2}{\sin^2 \theta_w \cos^2 \theta_w} \left(\frac{\mathcal{F}}{M_S^4} \right) \left(\frac{Q^2}{y} \right) \frac{1}{-Q^2 - M_Z^2} \left[g_a^e g_a^q (6y - 6y^2 + y^3) + g_v^e g_v^q (y - 2)^3 \right] \Big\} \\ & \left. + \frac{\pi}{2} f_g(x) \frac{Q^2}{sy^2} \left(\frac{\mathcal{F}}{M_S^4} \right)^2 \left(\frac{Q^2}{y} \right)^2 (1-y)(y^2 - 2y + 2), \right. \end{aligned} \quad (6)$$

where $Q^2 = sxy$ is the square of the momentum-transfer, $\sqrt{s} = 300$ GeV, and $f_{q/g}(x)$ are the parton distribution functions. The reduced amplitudes $M_{\alpha\beta}$ are given in Eq. (3) with s replaced by $-Q^2$. The last term in the above equation comes from the additional channel $e^+g \rightarrow e^+g$ allowed by the low scale gravity interactions. The channels $\sum_{\bar{q}} e^+ \bar{q} \rightarrow e^+ \bar{q}$ are also included. The HERA data [4] used in our analysis are shown in Table 1.

2.b Drell-yan at the Tevatron

CDF measured the double differential cross section $d^2\sigma/dM_{\ell\ell}dy$ ($\ell = e, \mu$) for the Drell-yan production, where $M_{\ell\ell}$ and y are, respectively, the invariant mass and the rapidity of the lepton pair. Essentially, CDF measured the cross section in the range $-1 < y < 1$ and then average over y to obtain the double differential cross section. The double differential cross section for $p\bar{p} \rightarrow \ell^+\ell^-$ is given by

$$\frac{d^2\sigma}{dM_{\ell\ell}dy} = K \left\{ \sum_q \left[\frac{M_{\ell\ell}^3}{72\pi s} f_q(x_1) f_{\bar{q}}(x_2) (|M_{LL}|^2 + |M_{LR}|^2 + |M_{RL}|^2 + |M_{RR}|^2) \right. \right.$$

$$+ \frac{\pi M_{\ell\ell}^7}{120s} f_q(x_1) f_{\bar{q}}(x_2) \left(\frac{\mathcal{F}}{M_S^4} \right)^2 \Big] + \frac{\pi M_{\ell\ell}^7}{80s} f_g(x_1) f_g(x_2) \left(\frac{\mathcal{F}}{M_S^4} \right)^2 \Big\}, \quad (7)$$

where $x_{1,2} = M_{\ell\ell} e^{\pm y} / \sqrt{s}$, $\sqrt{s} = 1800$ GeV, $f_{q,g}(x_i)$ are the parton distribution functions, and the sum over all possible $q\bar{q}$ pairs is understood. The reduced amplitudes $M_{\alpha\beta}$ ($\alpha, \beta = L, R$) are given in Eq. (3) with s replaced by $\hat{s} = M_{\ell\ell}^2$. The QCD K factor is given by $K = 1 + \frac{\alpha_s(\hat{s})}{2\pi} \frac{4}{3} (1 + \frac{4\pi^2}{3})$. The second term of the above equation comes from $q\bar{q} \rightarrow G \rightarrow \ell^+ \ell^-$ and the third one comes from $gg \rightarrow G \rightarrow \ell^+ \ell^-$. This K factor is, in principle, not valid for the gg channel, but it will not affect our calculation because we normalize our SM calculation to the expected number of events in each bin given by CDF when we deal with the CDF data (similarly, we normalize to the first bin of the D0 data when we deal with D0 data.) On the other hand, D0 measured the differential cross section $d\sigma/dM_{ee}$ with the rapidity range integrated. The Drell-yan data [5] we used in our analysis are shown in Table 2.

2.c LEPII fermion pair Cross sections

LEPII has measured the leptonic cross sections, hadronic cross sections, and heavy flavor (b and c) production. Since the low scale gravity interactions are naturally flavor-blind, we shall include the effects on all flavors here. For a massless q the expression for $\sigma(e^+e^- \rightarrow q\bar{q})$ is given by

$$\sigma(e^+e^- \rightarrow q\bar{q}) = K \left\{ \frac{s}{16\pi} (|M_{LL}|^2 + |M_{LR}|^2 + |M_{RL}|^2 + |M_{RR}|^2) + \frac{3\pi s^3}{80} \left(\frac{\mathcal{F}}{M_S^4} \right)^2 \right\}, \quad (8)$$

where the reduced amplitudes $M_{\alpha\beta}$ ($\alpha, \beta = L, R$) are given in Eq. (3), and the QCD K factor is $K = 1 + \alpha_s/\pi + 1.409(\alpha_s/\pi)^2 - 12.77(\alpha_s/\pi)^3$. The leptonic cross sections $\sigma(e^+e^- \rightarrow \mu^+\mu^-, \tau^+\tau^-)$ do not have this K factor. The LEPII data [6] used in our analysis are given in Tables 3 and 4.

2.d ν -N Scattering

The recent measurements by CCFR and NuTeV [7] are the most precise ones on the neutrino-quark couplings. Since the gravitons also couple to neutrinos, the measurements should, in principle, place a constraint on the scale M_S . However, the analysis by Rizzo in Ref. [2] showed that the constraint coming from these low energy ν -N scattering is very weak. This is because the center-of-mass energies of these collisions are only of order of tens of GeV's, even though the neutrino beam energy is as high as a few hundred GeV. In addition, the effective operators induced by the low scale gravity interactions are at least of dimension eight. This is in contrast to the traditional four-fermion contact interactions, which are only of dimension six. Therefore, at such low center-of-mass energies in these collisions, the effect of low scale gravity is extremely minimal. We are not going to include these data in our global fit.

3. Fits

For the fitting we follow the procedures in Refs. [8], where the four-fermion contact interactions are analyzed with a similar but larger global data set. The difference is that Refs. [8] include also the data sets from the low energy e -N scattering and the atomic parity violation, which constrain parity violating interactions. But the gravity is certainly parity conserving and thus it receives no restriction from these parity-violating experiments.

The interference effect between the SM amplitude and the low scale gravity scales as \mathcal{F}/M_S^4 , while the pure low scale gravity scales as $(\mathcal{F}/M_S^4)^2$. To linearize the fitting we use the parameter $\eta = \mathcal{F}/M_S^4$. We use MINUIT to minimize the χ^2 . The best estimates of η for each individual data set and the combined set are shown in Table 5. The SM fit gives a $\chi^2 = 86.66$ for 103 d.o.f., while the fit with non-zero η gives a $\chi^2 = 85.59$ for 102 d.o.f. Since the fits do not show any evidence for new physics, we can then place limits on the $\eta = \mathcal{F}/M_S^4$. The physical region of η is $\eta \geq 0$, and so we define the 95%CL upper limit for η as

$$0.95 = \frac{\int_0^{\eta_+} \mathcal{P}(\eta) d\eta}{\int_0^{\infty} \mathcal{P}(\eta) d\eta}, \quad (9)$$

where

$$\mathcal{P}(\eta) = \frac{1}{\sigma\sqrt{2\pi}} \exp\left(-\frac{\chi^2(\eta) - \chi^2_{\min}}{2}\right). \quad (10)$$

From η_+ we find the limits as $M_S/\mathcal{F}^{1/4} = \eta_+^{-1/4}$. The limits on $M_S/\mathcal{F}^{1/4}$ for each data set and the combined are also shown in Table 5. The combined limit is $M_S/\mathcal{F}^{1/4} > 970$ GeV, or

$$M_S > \begin{cases} 1150 \text{ GeV} & \text{for } n = 3 \\ 970 \text{ GeV} & \text{for } n = 4 \end{cases} \quad (11)$$

at 95%CL.

It is the Drell-yan production at the Tevatron that gives the strong constraint among all data. This is easy to understand because the \hat{s} of the Drell-yan process is the largest of all. The HERA data does cause a slight pull of the fit, about 1σ from zero, as shown by the last two rows in Table 5. The central value for the “ALL w/o HERA” fit is essentially zero but the “ALL” fit has a central value about 1σ from zero. We show in Fig. 1 the Drell-yan production for the SM and for the low scale gravity model with M_S and n given in Eq. (11), together with the D0 data.

To conclude, we have used the global lepton-quark neutral current data plus the leptonic cross sections at LEPII to constrain the low scale gravity interactions arising from the extra dimensions. The limit that we place on the effective Planck scale M_S is about 1.15 TeV for $n = 3$ and 0.97 TeV for $n = 4$ at 95%CL.

Acknowledgments

This research was supported in part by the U.S. Department of Energy under Grants No. DE-FG03-91ER40674 and by the Davis Institute for High Energy Physics.

References

- [1] N. Arkani-Hamed, S. Dimopoulos, G. Dvali, Phys. Lett. **B429**, 263 (1998); I. Antoniadis, N. Arkani-Hamed, S. Dimopoulos, and G. Dvali, Phys. Lett. **B436**, 257 (1998); N. Arkani-Hamed, S. Dimopoulos, G. Dvali, Phys. Rev. **D59**, 086004 (1999); N. Arkani-Hamed, S. Dimopoulos, J. March-Russell, SLAC-PUB-7949, e-Print Archive: hep-th/9809124.
- [2] G. Giudice, R. Rattazzi, and J. Wells, Nucl. Phys. **B544**, 3 (1999); S. Nussinov and R. Shrock, Phys. Rev. **D59**, 105002 (1999); E. Mirabelli, M. Perelstein, and M. Peskin, Phys. Rev. Lett. **82**, 2236 (1999); T. Han, J. Lykken, and R. Zhang, Phys. Rev. **D59**, 105006 (1999); J. Hewett, SLAC-PUB-8001, e-Print Archive: hep-ph/98011356; T. Rizzo, SLAC-PUB-8036, e-Print Archive: hep-ph/9901209; P. Mathews, S. Raychaudhuri, and K. Sridhar, TIFR-TH-98-51, e-Print Archive: hep-ph/9812486; P. Mathews, S. Raychaudhuri, and K. Sridhar, TIFR-TH-98-48, e-Print Archive: hep-ph/9811501; Z. Berezhiani and G. Dvali, NYU-TH-10-98-06, e-Print Archive: hep-ph/9811378; K. Agashe and N. Deshpande, e-Print Archive: hep-ph/9902263; M. Graesser, e-Print Archive: hep-ph/9902310; P. Nath and M. Yamagchi, e-Print Archive: hep-ph/9902323; M. Masip and A. Pomarol, e-Print Archive: hep-ph/9902467; K. Cheung and W.-Y. Keung, e-Print Archive hep-ph/9903294; T. Rizzo (SLAC). SLAC-PUB-8071, e-Print Archive: hep-ph/9903475; D. Atwood, S. Bar-Shalom, and A. Soni, e-Print Archive: hep-ph/9903538; C. Balázs, H.-J. He, W. Repko, C. Yuan, and D. Dicus, e-Print Archive: hep-ph/9904220; A. Gupta, N. Mondal, and S. Raychaudhuri, e-Print Archive: hep-ph/9904234; P. Mathews, S. Raychaudhuri, and K. Sridhar, e-Print Archive: hep-ph/9904232; K. Cheung, UCD-HEP-99-8, e-Print Archive: hep-ph/9904266; G. Shiu, R. Shrock, and S. Tye, ITP-SB-99-03, e-Print Archive: hep-ph/9904262; K. Lee, H. Song, J. Song, SNUTP-99-021, e-Print Archive: hep-ph/9904355; T. Rizzo, SLAC-PUB-8114, e-Print Archive: hep-ph/9904380; K. Yoshioka, KUNS-1569, e-Print Archive: hep-ph/9904433.
- [3] S. Cullen and M. Perelstein, SLAC-PUB-8084, e-Print Archive: hep-ph/9903422; L. Hall and D. Smith, LBNL-43091, e-Print Archive: hep-ph/9904267; N. Arkani-Hamed, S. Dimopoulos, N. Kaloper, and J. March-Russell, SLAC-PUB-8068, e-Print Archive: hep-ph/9903224; A. Mazumdar, IMPERIAL-AST-99-2-2, e-Print Archive: hep-ph/9902381; C. Csaki, M. Graesser, and J. Terning, LBNL-42952, e-Print Archive: hep-ph/9903319; T. Banks, M. Dine, and A. Nelson, e-Print Archive: hep-th/9903019.
- [4] H1 Coll., submission to ICHEP98, abstract no. 533; ZEUS Coll., submission to ICHEP98, abstract no. 752; L. Stanco, talk presented at ICHEP98, Vancouver, July 1998.
- [5] CDF Coll., Phys. Rev. Lett. **79**, 2198 (1997); D0 Coll., FERMILAB-PUB-98-391-E, e-Print Archive: hep-ex/9812010.
- [6] ALEPH Coll., CERN-EP/99-042 (March 1999); ALEPH-99-018 (March 1999), submission to 1999 winter conferences; DELPHI Coll., CERN-EP/99-05 (Jan 1999); L3 Coll., Phys. Lett. **B370**, 195 (1996); Phys. Lett. **B407**, 361 (1997); OPAL Coll., Eur. Phys. J. **C2**, 441 (1998); Eur. Phys. J. **C6**, 1 (1999);

OPAL Physics Note PN348 (July 1998), submission to ICHEP98, Vancouver, July 1998; OPAL Physics Note PN380 (March 1999), submitted to 1999 winter conferences; Seminar presented by D. Glenzibski at LEP2 Jamboree, March 1999.

- [7] CCFR Coll., Eur. Phys. J. **C1**, 590 (1998); NuTeV Coll., hep-ex/9806013.
- [8] V. Barger, K. Cheung, K. Hagiwara, and D. Zeppenfeld, Phys. Rev. **D57**, 391 (1998); K. Cheung, e-Print Archive: hep-ph/9807483; D. Zeppenfeld and K. Cheung, MADPH-98-1081, e-Print Archive: hep-ph/9810277.

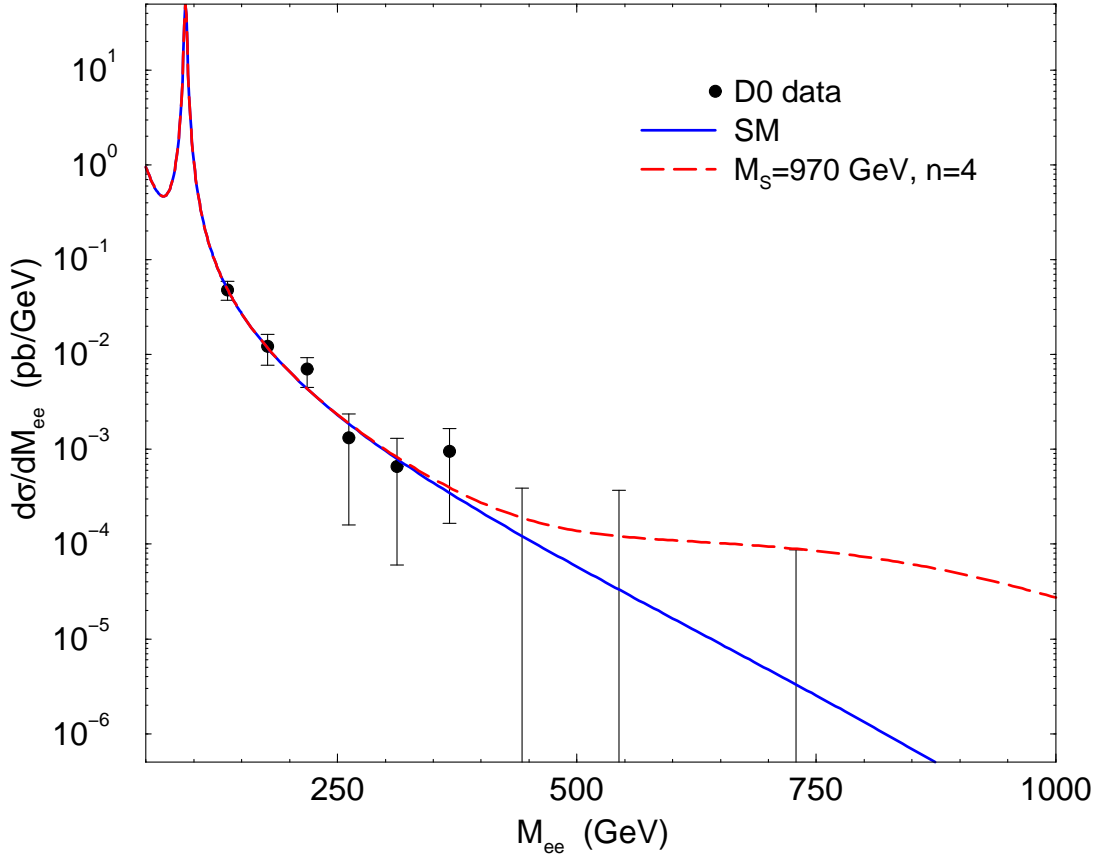


Figure 1: The differential distribution $d\sigma/dM_{ee}$ for Drell-yan production at the Tevatron for the low scale gravity model and for the SM. The data shown are from D0.

Table 1: The measured N_{obs} and expected N_{exp} number of events as a function of Q_{min}^2 at HERA.

ZEUS ($\mathcal{L} = 46.60 \text{ pb}^{-1}$)			H1 ($\mathcal{L} = 37.04 \text{ pb}^{-1}$)		
$Q_{\text{min}}^2 (\text{GeV}^2)$	N_{obs}	N_{exp}	$Q_{\text{min}}^2 (\text{GeV}^2)$	N_{obs}	N_{exp}
2500	1817	1792 ± 93	2500	1297	1276 ± 98
5000	440	396 ± 24	5000	322	336 ± 29.6
10000	66	60 ± 4	10000	51	55.0 ± 6.42
15000	20	17 ± 2	15000	22	14.8 ± 2.13
35000	2	0.29 ± 0.02	20000	10	4.39 ± 0.73
			25000	6	1.58 ± 0.29

Table 2: The Drell-Yan data by CDF and D0 [5]. N_{obs} is the observed and N_{exp} is the expected number of events.

CDF				
	e^+e^-		$\mu^+\mu^-$	
$M_{\ell\ell}$ (GeV)	N_{obs}	N_{exp}	N_{obs}	N_{exp}
50–150	2581	2581	2533	2533
150–200	8	10.8	9	9.7
200–250	5	3.5	4	3.2
250–300	2	1.4	2	1.3
300–400	1	0.97	1	0.94
400–500	1	0.25	0	0.27
500–600	0	0.069	0	0.087

D0	
	e^+e^-
$M_{\ell\ell}$ (GeV)	σ (pb)
120–160	$1.93^{+0.43}_{-0.44}$
160–200	$0.49^{+0.16}_{-0.18}$
200–240	$0.28^{+0.09}_{-0.10}$
240–290	$0.066^{+0.052}_{-0.058}$
290–340	$0.033^{+0.032}_{-0.030}$
340–400	$0.057^{+0.042}_{-0.047}$
400–500	< 0.063 (0.039)
500–600	< 0.060 (0.037)
600–1000	< 0.058 (0.035)

Table 3: The LEPII hadronic cross sections and the ratio R_b and R_c . Note that the cross sections given by ALEPH have an angular cut of $|\cos \theta| < 0.95$. The two sets of DELPHI data for R_b, R_c are given at $\sqrt{s} = 130 - 136$ and $161 - 172$ GeV, respectively. $\sigma_{\text{had}}^{\text{SM}}$ and $R_{b,c}^{\text{SM}}$ are the SM expectations.

\sqrt{s} (GeV)	σ_{had} (pb)	$\sigma_{\text{had}}^{\text{SM}}$ (pb)	R_b	R_b^{SM}	R_c	R_c^{SM}
ALEPH						
130	71.6 ± 3.96	70.7	0.176 ± 0.044	0.190	-	-
136	58.8 ± 3.61	57.3	0.214 ± 0.050	0.186	-	-
161	29.94 ± 1.84	30.7	0.159 ± 0.035	0.175	-	-
172	26.4 ± 1.75	25.1	0.134 ± 0.037	0.173	-	-
183	21.71 ± 0.74	21.1	0.176 ± 0.020	0.171	-	-
189	19.59 ± 0.46	19.3	-	-	-	-
DELPHI						
130.2	82.1 ± 5.2	83.1	0.174 ± 0.028	0.182	0.199 ± 0.073	0.225
136.2	65.1 ± 4.7	67.0				
161.3	40.9 ± 2.1	34.8	0.142 ± 0.024	0.165	0.314 ± 0.055	0.250
172.1	30.3 ± 1.9	28.9				
L3						
130.3	81.8 ± 6.4	78	-	-	-	-
136.3	70.5 ± 6.2	63	-	-	-	-
140.2	67 ± 47	56	-	-	-	-
161.3	37.3 ± 2.2	34.9	-	-	-	-
170.3	39.5 ± 7.5	29.8	-	-	-	-
172.3	28.2 ± 2.2	28.9	-	-	-	-
OPAL						
130.25	64.3 ± 5.1	77.6	-	-	-	-
133.17	-	-	0.195 ± 0.041	0.182	-	-
136.22	63.8 ± 5.2	62.9	-	-	-	-
161.34	35.5 ± 2.2	33.7	0.162 ± 0.041	0.169	-	-
172.12	27.0 ± 1.9	27.6	0.131 ± 0.047	0.165	-	-
183	23.7 ± 0.81	24.3	0.190 ± 0.022	0.163	-	-
189	22.1 ± 0.64	22.3	0.167 ± 0.014	0.162	-	-

Table 4: The LEPII leptonic cross sections for $e^+e^- \rightarrow \mu^+\mu^-, \tau^+\tau^-$. Note that the cross sections given by ALEPH have an angular cut of $|\cos \theta| < 0.95$. σ^{SM} are the SM expectations.

\sqrt{s} (GeV)	$\sigma_{\mu\mu}$ (pb)	$\sigma_{\mu\mu}^{\text{SM}}$ (pb)	$\sigma_{\tau\tau}$ (pb)	$\sigma_{\tau\tau}^{\text{SM}}$ (pb)
ALEPH				
130	7.9 ± 1.2	7.0	10.9 ± 1.8	7.3
136	6.9 ± 1.1	6.1	5.6 ± 1.3	6.3
161	4.49 ± 0.70	3.88	5.75 ± 0.99	4.01
172	2.64 ± 0.53	3.32	3.26 ± 0.75	3.43
183	2.98 ± 0.25	2.89	2.90 ± 0.30	2.98
189	2.66 ± 0.14	2.69	2.39 ± 0.16	2.78
DELPHI				
130.2	9.7 ± 1.9	8.1	10.2 ± 3.1	8.3
136.2	6.6 ± 1.6	7.0	8.8 ± 3.0	7.2
161.3	3.6 ± 0.7	4.5	5.1 ± 1.2	4.6
172.1	3.6 ± 0.7	3.8	4.5 ± 1.1	3.9
L3				
161.3	4.59 ± 0.84	4.4	4.6 ± 1.1	4.5
172.1	3.60 ± 0.75	3.8	4.3 ± 1.1	3.9
OPAL				
130.25	9.0 ± 1.8	8.0	6.8 ± 2.0	8.0
136.22	11.4 ± 2.1	7.0	7.2 ± 2.1	6.9
161.34	4.5 ± 0.7	4.4	6.2 ± 1.0	4.4
172.12	3.6 ± 0.6	3.8	3.9 ± 0.8	3.8
183	3.46 ± 0.29	3.45	3.31 ± 0.32	3.45
189	3.13 ± 0.16	3.21	3.53 ± 0.21	3.21

Table 5: The best estimate of the $\eta = \mathcal{F}/M_S^4$, 95%CL upper limit η_+ , and the 95%CL lower limit on $M_S/\mathcal{F}^{1/4}$.

Data Set	$\eta = \mathcal{F}/M_S^4$ (GeV $^{-4}$)	η_+ (GeV $^{-4}$)	95%CL $M_S/\mathcal{F}^{1/4}$
DY-CDF	$(0.00 \pm 0.15) \times 10^{-11}$	0.22×10^{-11}	819 GeV
DY-D0	$(0.00 \pm 0.12) \times 10^{-11}$	0.15×10^{-11}	907 GeV
DY-combined	$(0.00 \pm 0.10) \times 10^{-11}$	0.14×10^{-11}	924 GeV
LEPII hadronic	$(0.45^{+0.27}_{-1.18}) \times 10^{-11}$	0.87×10^{-11}	582 GeV
LEPII leptonic	$(-0.34^{+0.80}_{-0.68}) \times 10^{-11}$	1.01×10^{-11}	561 GeV
LEPII b,c	$(1.63^{+1.69}_{-5.87}) \times 10^{-11}$	4.42×10^{-11}	388 GeV
LEPII	$(-0.44^{+1.01}_{-0.29}) \times 10^{-11}$	0.74×10^{-11}	607 GeV
HERA	$(-0.32^{+0.16}_{-0.15}) \times 10^{-11}$	2.6×10^{-11}	443 GeV
ALL	$(-0.079^{+0.076}_{-0.051}) \times 10^{-11}$	0.11×10^{-11}	970 GeV
ALL w/o HERA	$(-0.0055^{+0.11}_{-0.10}) \times 10^{-11}$	0.14×10^{-11}	924 GeV